A&A 366, 796–810 (2001)
DOI: 10.1051/0004-6361:20000336

Astronomy & Astrophysics

Possible star formation in the halo of NGC 253⋆

F. Comerón[1], J. Torra[2], R. A. Méndez[3,4], and A. E. Gómez[5]

[1] European Southern Observatory, Karl-Schwarzschild-Str.2, 85748 Garching bei München, Germany
e-mail: fcomeron@eso.org
[2] Departament d'Astronomia i Meteorologia, Universitat de Barcelona, Av. Diagonal 647, 08028 Barcelona, Spain
e-mail: jordi@am.ub.es
[3] Cerro Tololo Inter-American Observatory, Casilla 603, La Serena, Chile
[4] European Southern Observatory, Casilla 19001, Santiago 19, Chile
e-mail: rmendez@eso.org
[5] Observatoire de Paris-Meudon, DASGAL, UMR 8633 du CNRS, 92195 Meudon Cedex, France
e-mail: ana.gomez@obspm.fr

Received 19 July 2000 / Accepted 28 November 2000

Abstract. We present a deep UBV survey in the direction of the halo of the starburst galaxy NGC 253 aimed at investigating the possible existence of recent star formation far from its disk, as traced by early-type stars. We discuss different classes of objects with blue colors that may contaminate the region of color-color and color-magnitude diagrams occupied by early Population I stars at the distance of NGC 253. Strong upper limits are found on their contribution to the measured object counts by means of models, of surveys of the halo of our Galaxy, and of observations of nearby control fields. A population of objects with $(B-V) < 0$, $V > 23$ is identified in the direction of the halo of NGC 253 that has no counterpart in the control fields to a high level of statistical confidence. The absolute magnitudes of these objects at the distance of NGC 253 is consistent with them being main sequence B0-B2 stars. The spatial distribution of the bluest objects in the halo of NGC 253 seems to cluster in two groups: one is closer to the disk of NGC 253, and may contain runaway stars expelled from its disk. The other group has projected distances to the plane of the galaxy ranging between 9 and 15 kpc, and at least its base coincides with a peak in radio continuum due to synchrotron emission of cosmic rays escaping the galactic disk. We hypothesize that the distant group of blue stars in the halo of NGC 253 is a result of the interaction between the superwind produced at its nuclear starburst (and perhaps also in star forming regions in the disk) and cold gas in the halo, in a phenomenon similar to the star formation near Centaurus A induced by the interaction of its jet with a HI cloud. If this is the case, NGC 253 provides an example of the ability of less energetic galactic outflows to trigger star formation in haloes, a phenomenon that may also be responsible for the suspected existence of Population I stars at large distances from the disk of the Milky Way.

Key words. stars: early-type – stars: formation – galaxies: halos – galaxies: NGC 253

1. Introduction

The existence of ongoing star formation in environments very different from massive molecular complexes in galactic disks is nowadays a fact supported by several lines of observational evidence. Indications of massive star formation in cooling flows falling on the cD galaxies in clusters is for instance deduced from their spectral characteristics in the ultraviolet (Crawford & Fabian 1993; Allen 1995; Smith et al. 1997). Conversely, evidence has been reported on star formation triggered by powerful radio jets from galactic nuclei, either in nearby clouds (Pinkney et al. 1996; van Breugel & Dey 1993) or in galaxies crossing the path of the jet (van Breugel et al. 1985; Best et al. 1997), although such interaction may be also disruptive in very low mass systems (Scannapieco et al. 2000). The nearest giant radio galaxy, Centaurus A, is such an example where the brightest individual stars can be observed (Graham 1998). Star formation in a HI cloud several kiloparsecs away from Centaurus A seems to be a consequence of the interaction of the radio-jets from the nucleus of the galaxy with the atomic and molecular gas (Schiminovich et al. 1994; Charmandaris et al. 2000) associated to its stellar shells, which are thought to have resulted from a past interaction with a disrupted companion.

Send offprint requests to: F. Comerón

⋆ Based on observations collected at the European Southern Observatory (La Silla, Chile), program 61.D-0447.

Star formation far away from the galactic plane has been suspected to be taking place at present, albeit at an extremely low rate, in the halo of our own Milky Way. Observed high-latitude early-type stars with apparently normal Population I spectra can be usually explained as runaway stars expelled from the galactic disk (Little et al. 1995; Rolleston et al. 1997, 1999), while detailed abundance analyses have shown that some are actually evolved, post-AGB stars (Mendoza & Arellano-Ferro 1993; Parthasarathy 1993; Hambly et al. 1996; Moehler & Heber 1998). However, a few objects remain whose high-resolution spectrum is fully compatible with Population I membership, while their implied large distances to the galactic plane makes it necessary to invoke in situ formation (Brown et al. 1989; Conlon et al. 1992; Hambly et al. 1993; Little et al. 1995). Extraplanar ionized gas extending up to several kiloparsecs from the galactic plane, observed through Hα emission in edge-on galaxies (Pildis et al. 1994; Donahue et al. 1995; Hoopes et al. 1999; Rossa & Dettmar 2000), might be related to star formation in such environments. Star formation in a low-density medium is also observed in the bridge joining the two Magellanic Clouds (Demers et al. 1991; Grondin et al. 1992).

The widely different scenarios of star formation just mentioned may reflect a variety of ways in which star formation can be triggered in the haloes of galaxies. In the first two examples given above, the driving agent of star formation can be identified with large-scale compressions produced by high velocity streams of gas, either inflows or outflows, encountering obstacles in their path. In the case of the Milky Way the mechanisms and even the observational evidence are more controversial. Dense clumps in high velocity clouds (Wakker & van Woerden 1997; Combes & Charmandaris 2000) may be sites of star formation, perhaps triggered by collisions among them (Dyson & Hartquist 1983). However, the evidence for star formation in high velocity clouds is tentative at most (Ivezic & Christodoulou 1997; Christodoulou et al. 1997).

NGC 253 is a well studied nearly edge-on Sc-type galaxy in the Sculptor group. Several reasons make it a well suited object to explore potential mechanisms able to trigger star formation in the haloes of spiral galaxies. In the first place, its proximity to us puts any possible O and early B type stars in its halo within the reach of medium- and large-sized telescopes, making it possible to establish a census of this population, while its nearly edge-on inclination allows a straightforward separation between the halo and disk populations. Secondly, its location in the sky near the Southern galactic pole minimizes the density of foreground blue Population II stars in our Galaxy, whose colors can be similar to those of the objects in which we are interested. A third factor of importance concerns the combination in NGC 253 of a nuclear starburst (Lehnert & Heckman 1995, 1996) and a fairly intense star forming activity all over its disk (Sofue et al. 1994). This suggests a considerable level of disk-halo interaction if massive stars in the disk are responsible for powering the circulation of gas between the disk and the halo (Mac Low 1999). As such, NGC 253 may be regarded as an intermediate example, in terms of power injection into the halo, between radio galaxies having AGN-powered relativistic jets and "normal" galaxies lacking an energetic central engine.

The detection and location of blue stars in the halo of NGC 253 could thus provide important clues on the relative importance of starburst-driven galactic superwinds and of chimneys in the galactic disk drilled by OB associations in triggering star formation in galactic haloes. On the other hand, their non-detection would suggest that a vigorous disk-halo interaction is not sufficient to produce any significant star formation in the halo. This may in turn be interpreted as an indication that these stars are also likely to be absent from the halo of the Milky Way, and that the apparent halo Population I stars found in our Galaxy may not be really young massive stars. An investigation based in this approach has been already carried out by Hambly et al. (1995) on M 31, a galaxy whose features are closer to those of the Milky Way, with some tentative detections.

In this paper we present the results of a search for blue stars on a large fraction of the halo of NGC 253, and discuss the evidence for the existence of a significant number of faint blue objects with UBV magnitudes consistent with them being early-type Population I stars at the distance of NGC 253. Our observations are presented in Sect. 2. Section 3 discusses the results and the possible contributors to the star counts at faint blue magnitudes. Section 4 presents the statistical evidence for an excess of blue sources in the direction of the halo of NGC 253 and the arguments in support of their Population I nature, dealing also with their spatial distribution, their possible origin, and suggestions for further observations. Our conclusions are presented in Sect. 5.

2. Observations and data reduction

Our observations were carried out using the SUSI2 imager at the ESO New Technology Telescope (NTT) on the nights of 26 and 27 August 1998. The time allocated to our project allowed us to image seven overlapping fields covering 198 arcmin^2 southeast of NGC 253 in the U, B, and V filters. The area observed is shown in Fig. 1 outlined on a Digitized Sky Survey image of the field around NGC 253. Three exposures per field and filter were obtained, slighly offsetting the telescope after each exposure. This allowed us to correct for bad pixels in the detectors, to remove cosmic ray hits, and to cover the gap between the two chips composing the detector of SUSI2. Total exposure times were 60 min in U, 40 in B, and 40 in V. In addition, two control fields were observed using the same strategy and exposure times as for the halo fields, in order to have a representative sampling of the foreground and background population of objects in that direction of the sky. These control fields lie approximately 3° away from NGC 253, and were chosen at random with the only constraints of being far from any other galaxy of the Sculptor group and of not containing any stars with $V < 15$ that

Table 1. Coordinates of the centers of the two observed control fields and of NGC 253

Field no.	α (2000)	δ (2000)
1	0:49:00.0	−22:49:30
2	0:48:00.0	−22:49:45
NGC 253	0:47:33.2	−25:17:17

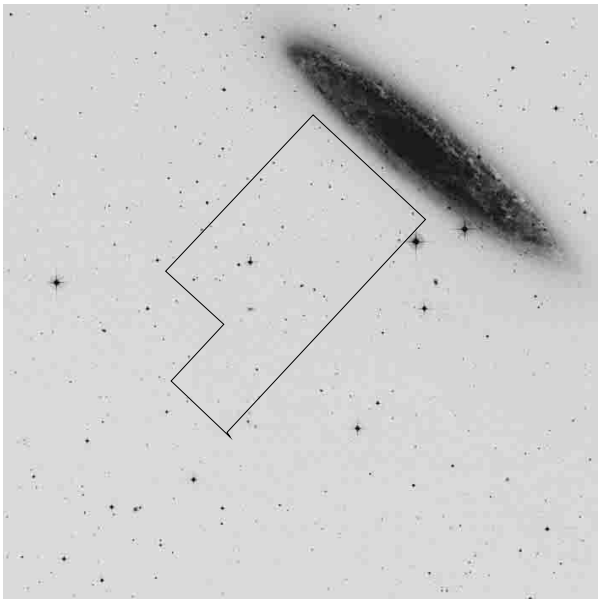

Fig. 1. A Digitized Sky Survey image of the field southeast of NGC 253 outlining the area that we observed with the NTT. The field shown here is $40' \times 40'$ in size, with North at the top and East to the left

could saturate the detector. Together they sample an area of 59 arcmin^2. The coordinates of the centers of the control fields, as well as those of the center of NGC 253 for reference, are given in Table 1.

The reduction of the images was performed using standard IRAF tasks and dedicated IRAF scripts. The bias level of each frame was determined by averaging the pixel values of the prescan and the overscan at each row and for each chip separately. This is the procedure recommended for bias subtraction of SUSI2 images, given that the bias level at a given row varies with the illumination. Pixel-to-pixel variations were corrected by ratioing the frames by dome flat fields. Ratioing by twilight sky flat fields was tried too, but this was found to leave a difference in the background count level between the center of the frames and the edges, at the 4% level in the V filter. This effect was removed when ratioing by dome flats instead. However, dome-flat fielded frames still exhibit a slight background slope across the frames, with a magnitude of 4% of the central illumination level between the extremes of the slope for the V filter. The percent increases to 6% in B and 8% in U, while the pattern remains constant in appearance and scale in all the frames taken through a given filter. In raw (non flat-fielded) frames the slope is seen to be even larger (11% in V). This behavior seems to exclude shutter delay in the flat fields as a possible cause of the gradient. On the other hand, the overlap among the fields allowed us to check for possible systematic differences in the CCD response between the two extremes of the slope which might in principle be responsible for the gradient. Allowing for the differences in zeropoints between each of the overlapping frames (which were calculated as explained below, using reference stars without any preference for any particular area of the field), no systematic effects in the magnitudes were found dependent on the position of the star in the detector, thus leading us to assume that the response of the CCD is uniform despite of the existence of the gradient in background. Therefore, we forced the removal of the gradient by fitting and subtracting a low-order polynomial to each image. We noticed that this procedure also removed part of a real gradient of illumination in the V-filter frames near the base of the halo of the galaxy, produced by the outskirts of the disk of NGC 253. The bias-subtracted, flat-fielded, and gradient-subtracted frames of each field were then shifted and combined, using the positions of reference stars in each frame to determine the relative shifts. Deviant pixels were identified and removed in the combination process.

Object detection and photometry were carried out on each combined frame individually, making use of different tasks in the DAOPHOT package (Stetson 1987). The details of our procedure are as follows: in the first place, an estimate of the sky level and its noise were obtained by iteratively calculating the median and the standard deviation of the pixel distribution. We rejected the pixels at more than 3σ from the median at each iteration in order to exclude both remaining cosmic rays and real objects from the calculation of the sky median. Next, a bright and isolated star was chosen in each frame to derive the point spread function (PSF), that was fitted with a Gaussian using the DAOPHOT task PSF. Measurements of the PSF for stars in different parts of the field of view did not show any significant changes, so spatial variations in the PSF parameters were not considered. The full width at half maximum (FWHM) of the Gaussian was used to define an optimal set of input parameters for the task DAOFIND, in particular the width of the convolution kernel. The limits on the sharpness and roundness parameters measured on the detected objects were set so as to exclude cosmic rays that may not have been filtered out at the image reduction stage, as well as clearly extended objects. Then, DAOFIND was executed using a threshold for detection of 3 times the standard deviation of the sky background counts previously determined. A comparison between the images and the list of detected objects showed that the chosen threshold still allowed many spurious detections, especially near the edges of the fields that were not imaged by all the individual exposures, leading to a higher sky noise. However, rising the threshold to a value like 5σ was found to miss some clear detections near the faint end, and we preferred to keep the low threshold value. This was not a real problem, as the very large photometric errors of

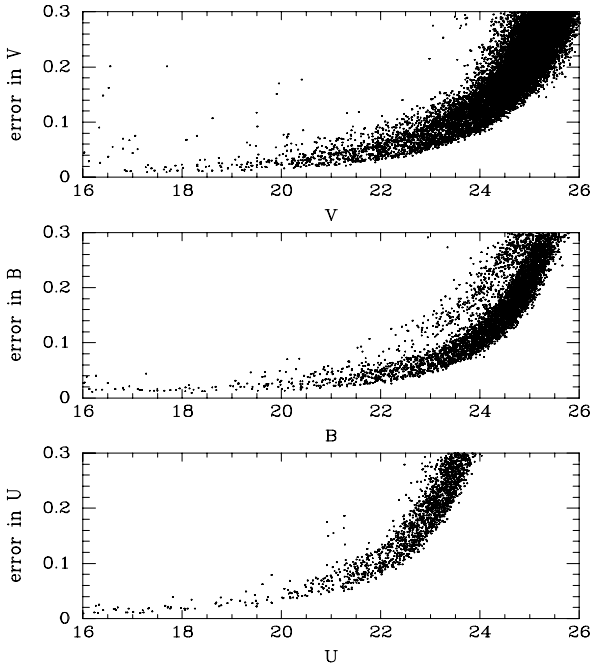

Fig. 2. Photometric errors in each band as a function of the magnitude, for both halo and control fields. The somewhat deviant points in the diagram for the B filter correspond to one of the halo fields

barely detected objects and spurious detections excluded them from the further analysis presented in this paper.

Preliminary aperture photometry, which is needed by the DAOPHOT PSF fitting tasks, was performed by running PHOT on the list of detected objects, setting the aperture and sky annulus parameters according to the FWHM value found earlier. After this, PSF-fitting instrumental photometry was performed using the DAOPHOT task PEAK. The sharpness parameter (defined in a somewhat different way as in DAOFIND) and the chi parameter measuring the goodness of the fit were used to exclude extended objects and cosmic rays that may not have been recognized as such by DAOFIND.

The conversion of the instrumental photometry to the Johnson UBV system was based on the photometric sequence in the field of NGC 253 defined by Alcaino & Liller (1984). Since these stars are in general bright and saturated in our long exposures, we had to define a set of fainter secondary standards in each observed field, both in the halo of NGC 253 and in the control fields. To this end, we obtained a series of short exposures in each filter centered on the fields containing the Alcaino & Liller standards, then the halo fields, then the control fields, and then the fields with the standards again. These series were obtained when the telescope was pointing near the meridian, so as to minimize the airmass changes during the exposures. In this way, we could tie the instrumental photometry of the secondary standards defined in each field to that of the bright standards defined by Alcaino and Liller. To convert the instrumental magnitudes into Johnson UBV magnitudes, we took into consideration color terms in the transformation equations, which are known to be significant at least in the B filter used with SUSI2. We determined the color terms by observing ten Landolt (1995) standard fields imaged at different airmasses, and applying the equations

$$U = u' - k_U X + k'_U(u' - b') + Z_U \quad (1a)$$

$$B = b' - k_B X + k'_B(b' - v') + Z_B \quad (1b)$$

$$V = v' - k_V X + k'_V(b' - v') + Z_V \quad (1c)$$

where U, B, V are the system magnitudes, u', b', v' are the instrumental magnitudes, k_U, k_B, k_V are the extinction coefficients, X is the airmass, k'_U, k'_B, k'_V are the color terms in each band, and Z_U, Z_B, Z_V are the corresponding zeropoints. The obtained color terms were $k'_U = 0.011$, $k'_B = -0.120$, and $k'_V = 0.005$, in good agreement with independent measurements published in the NTT webpages. It should be pointed out that the standard sequence of Alcaino and Liller in NGC 253 does not include stars bluer than $(B - V) = 0.51$, $(U - B) = -0.01$, and therefore does not bracket the color ranges of the blue objects of interest in the present work. The same is true for the stars in the observed Landolt fields, whose color ranges are $0.6 < (B - V) < 2.3$ and $0.0 < (U - B) < 2.3$. Slight systematic color effects thus may not be ruled out, although they should affect in the same way both the halo and the control fields.

With the color terms in hand, we then proceeded to find the zeropoints in the short exposures of our photometric sequences. This can be done using a set of transformation equations simpler than Eqs. (1), due to the fact that these observations were obtained at very nearly the same airmass and therefore the term containing X can be absorbed into modified zeropoints: $Z'_U = Z_U - k_U X$, $Z'_B = Z_B - k_B X$, $Z'_V = Z_V - k_V X$. The instrumental magnitudes in the photometric calibration exposures (u', b', v') and those in the deep exposures (u, b, v) are simply related by $u = u' + S_u$, $b = b' + S_b$, $v = v' + S_v$, where the zeropoints S_u, S_b, S_v may be expected to vary slightly for each field due to the varying sky conditions during the observing run. In this way, we obtain the transformation equations that we used:

$$U = u + k'_U(u - b) + [Z'_U - S_u - k'_U(S_u - S_b)] \quad (2a)$$

$$B = b + k'_B(b - v) + [Z'_B - S_b - k'_B(S_b - S_v)] \quad (2b)$$

$$V = v + k'_V(b - v) + [Z'_V - S_v - k'_V(S_b - S_v)]. \quad (2c)$$

Finally, astrometry was performed on each field by identifying point sources common to the USNO catalog.

The main output of our data reduction is a catalog of positions and UBV magnitudes of point sources detected in each field. Probable errors of 0.2 mag are typically reached at $U = 23.0$, $B = 25.0$, $V = 24.5$, with some variations from field to field as shown in Fig. 2. For the analysis presented in this paper, we retained only those objects detected in both B and V, and having a probable error $\epsilon(B - V) < 0.2$ mag. We did a final selection of objects by visually inspecting the images of each detected

source fulfilling these criteria, and discarding those objects that were clearly extended or that appeared superimposed on bright extended sources. No detailed experiments were carried out to assess the completeness level of the sample defined in this way at different magnitude and color limits, as the focus of this paper is on a differential comparison between the characteristics of the halo and control fields. However, given the relevance of slightly different completeness limits among the imaged fields with regard to the conclusions of this paper, numerical experiments with artificial stars were carried out and are described in Sect. 4.1

3. Results

The large number of point sources detected in the direction of the halo of NGC 253 can be divided into three broad categories: a foreground component made of high latitude objects in our own galaxy, a background component contributed by extragalactic objects of a variety of natures and at different redshifts, and a genuine population of objects belonging to the halo of NGC 253. As a first approximation, galactic structure models, large area multicolor surveys, and deep fields in small areas of the sky can be used to estimate the contribution of the first two kinds of objects to the sources detected in our observations. Such estimates are however prone to different theoretical and observational uncertainties, especially when reaching down to the faint magnitudes under consideration here. Effects such as the poorly known faint end of the stellar mass function, or density and luminosity evolution of objects at high redshift, introduce considerable uncertainties on the expected numbers of objects and their color distributions in the magnitude range where we may expect to detect members of the halo of NGC 253. Actual photometric surveys with follow-up spectroscopy of large fields (e.g. Hall et al. 1996) or deep fields such as the Hubble Deep Fields (HDFs) (e.g. Conti et al. 1999) are helpful in providing actual counts of field objects in different color regimes, but for the purposes of this paper they are limited by their relatively bright magnitude cutoffs and by their very limited areal coverage, respectively. For these reasons, it is essential to have an independent, empirical assessment on the actual distribution of foreground and background objects in color and magnitude with the same completeness characteristics as the survey of the halo of NGC 253 that we are discussing here. Our control fields, which sample both the foreground and background populations at essentially the same galactic longitude and latitude, provide this model- independent assessment on the significance of the excess of blue objects.

Color-magnitude and color-color diagrams are presented in Figs. 3 to 6. Figures 3 and 5 show the overall distribution of objects both in the halo fields and in the control fields, while Figs. 4 and 6 zoom into the regions occupied by faint blue objects of interest here. In the rest of this section, we briefly describe the main expected contributions in different regions of these diagrams. The discussion on the possible population of the halo of NGC 253 is based on an assumed distance modulus $DM = 27.06$ mag to this galaxy, which is the average of different methods used by Puche & Carignan (1988) and corresponds to a distance of 2.6 Mpc. The uncertainty in the distance modulus, ± 0.6 mag, is compatible with other determinations found in the literature (Graham 1982; Davidge & Pritchet 1990; Davidge et al. 1991). We have made no correction for foreground reddening, which is nearly insignificant in the direction of NGC 253 ($A_B = 0.04$; Tully 1988).

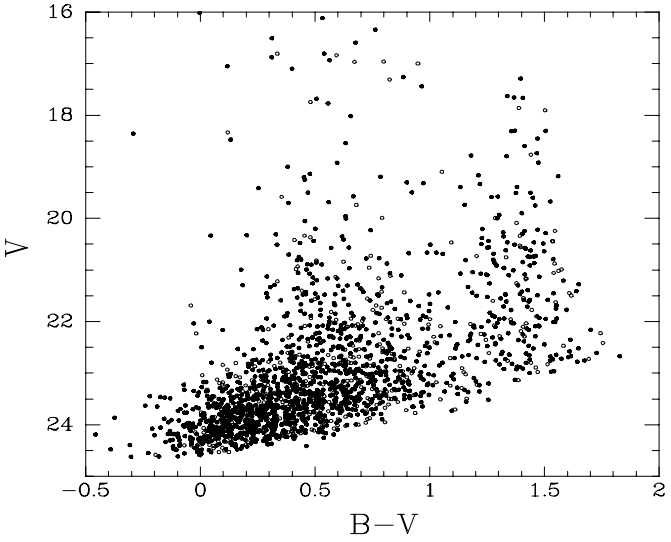

Fig. 3. $(B - V)$, V diagram of point sources detected in our survey. Full circles correspond to the NGC 253 halo fields, and open circles to the control fields

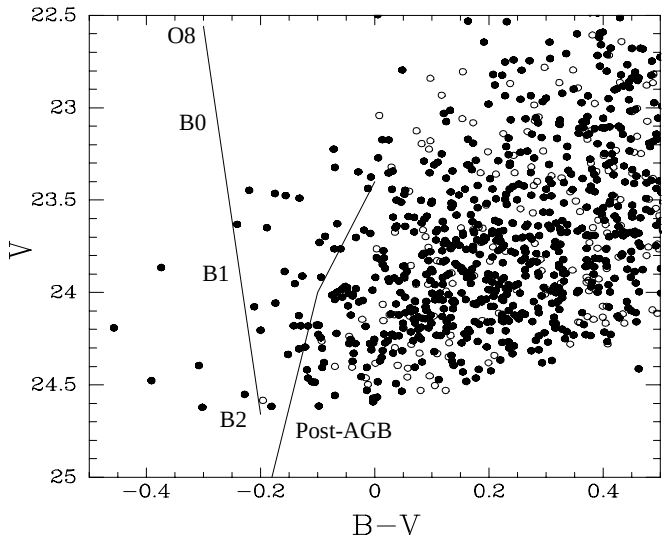

Fig. 4. A zoomed view of the $(B-V)$, V diagram presented in Fig. 3, showing in detail the distribution of sources in the region of the color-magnitude diagram where young halo objects in NGC 253 may lie. Full circles correspond to the NGC 253 halo fields, and open circles to the control fields. The lines mark the approximate locus expected for early-type Population I stars of different types and blue post-AGB stars at the adopted distance of NGC 253

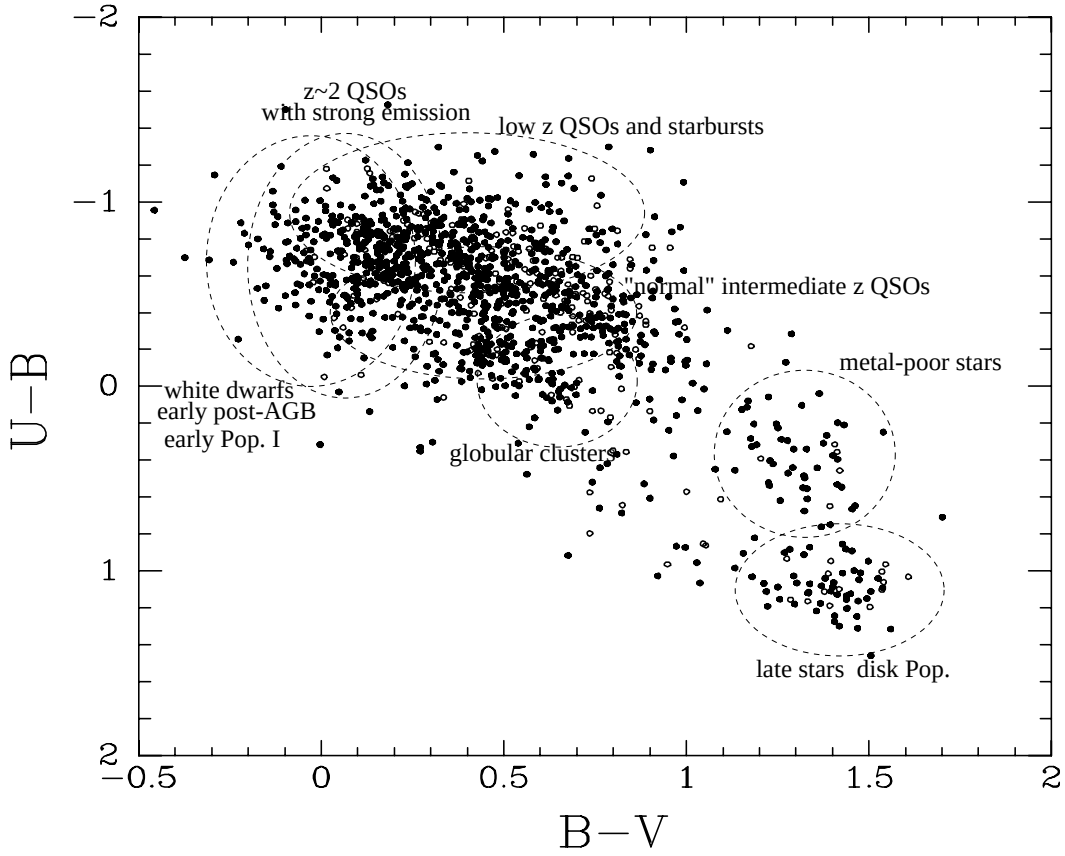

Fig. 5. $(B-V)$, $(U-B)$ diagram of point sources detected in our survey. Symbols are the same as in Figs. 3 and 4. The classes of objects that may be expected to populate the different regions of the diagram, as described in Sect. 3, are roughly indicated in figure

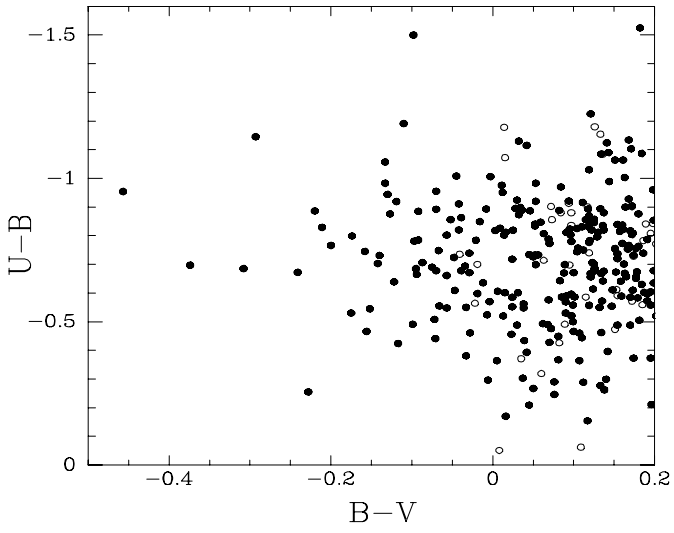

Fig. 6. A zoomed view of the $(B-V)$, $(U-B)$ diagram presented in Fig. 5, showing in detail the distribution of sources in the region of the color-color diagram where young halo objects in NGC 253 may lie. Symbols are the same as in Figs. 3 to 5

3.1. The galactic foreground population

3.1.1. The bulk stellar component

The brighter magnitude bins of our sample are expected to be dominated by the stellar component of our Galaxy, and the distribution of objects in the brighter parts of the color-magnitude diagram of Fig. 3 (above $V \sim 22$) is qualitatively similar to wide area surveys at high galactic latitudes (see for instance Stobie & Ishida 1987). The stellar component is mainly distributed along two vertical strips in the $(B-V), V$ diagram of Fig. 3, centered approximately at $B-V = 0.6$ and $B-V = 1.4$. The double-peaked appearance of the $B-V$ distribution for $V > 17$ is a well known feature where the bluer and the redder peaks are dominated by the spheroid and the disk populations respectively (Yoshii et al. 1987). The red peak in $B-V$ is in turn split into two components when plotting it in the $(B-V)$, $(U-B)$ diagram, with rough centers near $U-B = 0.4$ and $U-B = 1.1$. This is a feature found by Stobie & Ishida (1987) as well: the increasing numbers of relatively blue objects in $U-B$ for a given $B-V$ are attributed to the increasing contribution of metal-poor stars to star counts when going to fainter magnitudes. The star count models of Yoshii et al. (1987) predict a dominant contribution of solar-metallicity stars down to $V = 24$ in that range of $B-V$, in apparent contradiction with the similar importance of both clumps in Fig. 5. The discrepancy can be explained by the larger number of metal-rich objects that are missing in the color-color diagram at faint magnitudes due to their non-detection in U, as the $U \sim 23.5$ limit of our survey implies a two-color detection threshold that is brighter by $V \sim 0.7$ mag for metal-rich red stars than for metal-poor blue stars.

3.1.2. High latitude blue stars

Of special interest in the context of the present work is the possible contamination by faint objects with blue colors similar to those of Population I stars, namely hot subdwarfs, blue horizontal branch stars, and white dwarfs. Recent determinations of midplane space densities and scale heights for the first two classes of objects (Villeneuve et al. 1995; Sluis & Arnold 1998) predict essentially zero such objects in the area of our survey. On the other hand, star count models (Méndez 1995) predict approximately 2 white dwarfs in the area of the survey down to $V = 24.5$, although this result may be affected by uncertainties in the distribution of these objects perpendicular to the galactic plane. The intriguing possibility of the existence of a numerous population of old, faint and blue white dwarfs recently suggested by studies of the Hubble Deep Fields (Ibata et al. 1999; Méndez & Minniti 2000) is not likely to substantially modify this estimate, as the objects identified so far have $B-V > 0$. In any case, white dwarfs are the only potential source of contamination at $B-V < 0$, and indeed a clear white dwarf candidate appears in the halo fields with $V = 18.36, B-V = -0.29, U-B = -1.15$ (see Fig. 10).

3.2. The extragalactic background population

3.2.1. QSOs and AGNs

The main contribution to the faint blue region of the color-magnitude diagrams is expected to come from background QSOs and AGNs (e.g. Braccesi et al. 1980; Cristiani et al. 1989; Hall et al. 1996; Scholz et al. 1997). The colors of such objects have large variations due to their intrinsic spectral energy distributions, the relative intensity of their emission lines and, very importantly, their redshift. Low redshift QSOs have negative $U-B$ colors, but tend to be relatively red in $B-V$ due to the presence of [OIII] and Hβ in the V band. At higher redshifts the Balmer continuum moves from the B to the V bands, and some strong ultraviolet lines (MgII λ2798 Å, CIII] λ1909 Å, CIV λ1549 Å) enter successively the B band, producing as a result a steady bluening of the $B-V$ color. The $U-B$ color peaks at its most negative value near $z = 1.8$ as Lyα enters the U band, and decreases afterwards as the shorter wavelength flux is suppressed by the Lyα forest. For QSOs with a shallow spectral index and strong emission lines, the position in the $B-V$, $U-B$ diagram may be indistinguishable from that of early-type stars; these objects are thus our main concern at the time of detecting the signature of a population of blue stars in the halo of NGC 253. At $z > 2.3$, the redshift of CIV and then Lyα into the V band and the progressive entry of the Lyα forest into the B band contribute to redden $B-V$, so that QSOs move into the region of the $(B-V),(U-B)$ diagram occupied by mid-type stars, while their fainter apparent magnitudes removes them from sight in our survey.

3.2.2. Starbursts

Compact narrow emission-line galaxies at low redshift also contribute to ultraviolet excess-selected samples. However, as pointed out by Hall et al. (1996) (see also Cristiani et al. 1989), they are generally well separated from QSOs due to their redder $B-V$ because of their strong redshifted emission lines, particularly the Balmer lines. None of such objects in the Hall et al.'s survey enter the region of the $(B-V),(U-B)$ diagram of interest here. Such objects may be the brighter counterparts of the compact blue population detected in the Hubble Deep Fields (Elson et al. 1996; Méndez et al. 1996) that Elson et al. (1996) tentatively classified as distant starbursts. As already mentioned in the previous section, some recent evidence suggests that at least some of these objects may be galactic old white dwarfs, but their trend to appear near resolved galaxies (Elson et al. 1996) supports their extragalactic nature.

The color-magnitude and color-color diagrams in Figs. 3 to 6 show indeed a large abundance of faint, blue point sources in both the halo and the control fields. However, as clearly seen in Figs. 4 and 6, objects with extreme colors are considerably more abundant in the halo fields than in the control fields, what leads us to deduce a real difference between both. We attribute this difference to the presence of blue objects in the halo of NGC 253; the evidence for an excess density of blue objects in the halo fields is discussed in the next sections.

3.3. The intrinsic population of the halo of NGC 253

3.3.1. Globular clusters

The only stellar component resolved so far in the halo of NGC 253 are the brightest members of the asymptotic giant branch (Davidge & Pritchet 1990). These objects are near our detection limit at V and far below it at B, so we will not consider them here. On the other hand, globular clusters at the distance of NGC 253 are expected to have angular sizes below $1''$, and should therefore appear as stellar in our observations. For a typical integrated magnitude $M_V \simeq -7$ to -10, they should have $V \simeq$ 17–20 at the adopted distance of NGC 253, well within our detection limits. Unfortunately, their colors in the $(B-V),(U-B)$ diagram are virtually indistinguishable from those of mid- to late-G metal poor stars in the Milky Way halo, whose apparent magnitudes are also expected to be in that same range for heliocentric distances of a few kiloparsecs. Moreover, that color range may also be populated by $z > 3$ QSOs, although the latter should be fainter in the average. The wide range of distances to the plane of NGC 253 covered by our images should sample both bulge and halo globular clusters, with the subsequent spread in both metallicity and colors and therefore diluting even further their possible signature in color-color and color-magnitude diagrams. Indeed, adopting the color-metallicity relationship for galactic globular

clusters of Barmby et al. (2000) we find seven candidates with $17 < V < 20$ in the halo fields, and four objects occupying the same region of the color-color-magnitude diagram in the control fields, which is compatible with all such objects in the direction of the halo of NGC 253 being different from globular clusters.

3.3.2. Post-AGB stars

Population II post-AGB stars may also be individually detected at the distance of NGC 253. The brightest of these objects are expected to evolve from the AGB towards the blue at a nearly constant luminosity of $\log L(L_\odot) \simeq 3.4$ (Dorman et al. 1993), reaching temperatures of up to 10^5 K and very blue colors. Bright, blue post-AGB stars have very short lives (several times 10^4 years), but the fact that their progenitors are the abundant solar-mass stars implies a considerable number of bright, blue post-AGB stars observable in a galaxy at any given time. The upper limit in their luminosity is fairly insensitive to metallicity for metal-poor post-AGB stars, and this has lead Bond & Fullton (1997) to propose the use of the brightest post-AGB stars as standard candles for nearby galaxies.

The brightness and blue color of hot post-AGB stars makes them a potential source of confusion with Population I stars in the halo of NGC 253. Furthermore, and unlike in the case of other blue objects discussed so far, they should be found only in the halo fields and not in the control fields, making it difficult to disentangle their relative contribution from that of real Population I stars if both are present. Fortunately for our purposes, the bolometric corrections for post-AGB stars in the color range of interest in this work are important and rapidly increase towards the blue, and post-AGB stars may be expected to vanish below our detection limit in the region of posible confusion. Adopting standard $B-V$ vs. bolometric correction calibrations for supergiants (Schmidt-Kaler 1982) and the distance modulus discussed at the beginning of Sect. 3, we obtain $V = 23.4$ at $B - V = 0$ for the brightest post-AGB stars, dropping rapidly to $V = 24.0$ at $B-V = -0.1$ and $V = 25.2$ at $B-V = -0.2$. The adoption of the supergiant calibration for these object appears to be justified by their similarly low surface gravity. Moreover, recent model atmospheres at different surface gravities and metallicities (Castelli 1999 and references therein) indicate that the influence of metallicity (much lower in Population II post-AGB stars than in Population I supergiants) on the bolometric correction appears to be negligible in the temperature range of interest here, and in any case would make the V magnitudes estimated above only ∼0.1 fainter.

Although in principle the detectable post-AGB stars should thus be redder than early-type Population I stars, two reasons make it necessary to take this conclusion with caution. In the first place, as discussed in Sect. 2, photometric errors in $B-V$ reach typically 0.2 mag at $V = 24.5$. Therefore, some post-AGB stars with $B-V \simeq 0$ may have been plotted at $B - V$ of up to -0.2 in Figs. 3 and 4 by virtue of the uncertainty in the photometry. Secondly, as briefly discussed at the beginning of Sect. 3, uncertainties subsist as to the distance modulus of NGC 253, and a brightwards shift in the estimated V magnitudes of its post-AGB stars of up to ∼0.5 mag may not be entirely ruled out. We will further discuss these concerns in Sect. 4.

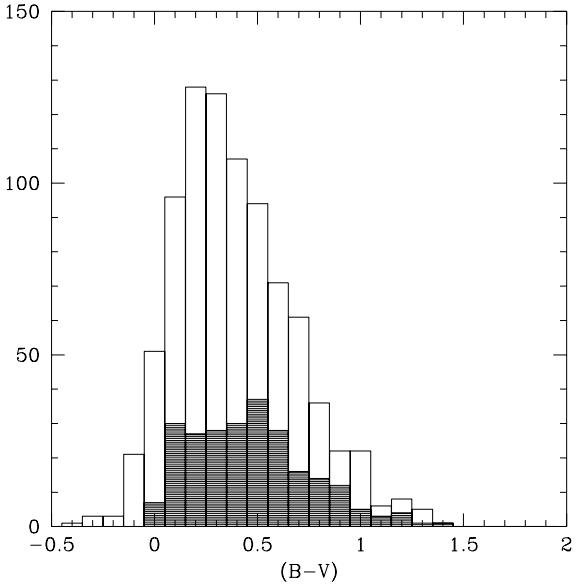

Fig. 7. Histogram of the $(B - V)$ color distribution of sources in the NGC 253 halo fields (blank bars) and the control fields (shaded bars). Besides the overall scaling factor due to the ratio of surveyed areas in each case, there is a rather sharp cutoff in the color distribution for control fields that is replaced by a blue tail in the case of the halo fields. Only stars with magnitudes $23.0 < V < 24.5$ have been included in the histogram

Finally, the observed magnitudes and colors of the objects with $B - V < 0$ appearing at $V > 23$ are similar to what would be expected for early B stars at the distance of NGC 253. In the region of $V \simeq 23.5$, $B-V = -0.2$, where the typical error in $B-V$ is about 0.12 mag, no post-AGB stars of NGC 253 should appear, and the most plausible explanation for the objects appearing there seems to be either QSOs or early-type Population I stars. The evidence for their true Population I character is discussed in Sect. 4.

4. Discussion: Population I component in the halo of NGC 253?

4.1. The excess of faint blue sources in (B − V), V diagram and its statistical significance

Figure 7 compares the distribution of $B - V$ colors in the magnitude interval $23 < V < 24.5$, namely the range where we identify a "blue tail" in the $(B-V), V$ diagram, especially in the halo fields. A visual inspection of the figure shows that the overall distribution of point sources in the halo is somewhat skewed towards bluer magnitudes than that of the control field sources. Moreover, the distribution of $B - V$ in the control fields drops rather sharply bluewards of $B - V = 0.1$ with only 7 objects bluer than

$B - V = 0.05$, while there are 79 such objects in the halo fields, i.e. a factor of 3.4 higher than would be expected from the ratio of surveyed areas in the halo and the control fields. A comparison between the distribution of photometric errors at faint magnitudes shows that this difference cannot be due to different completeness degrees between halo and control fields. Differences in completeness among the fields at a given magnitude set by the condition $\epsilon(B - V) < 0.2$ mag (Sect. 2) are suggested by deviations in the run of data for different individual fields in Fig. 2. However, a closer inspection of these differences (especially those in the B filter, where the deviant behaviour of one of the halo fields is more apparent) indicates that the control fields are slightly *deeper* on the average.

Given the decisive role that a uniform degree of completeness at these faint magnitudes has in our claim of an apparent excess of blue sources in the direction of the halo of NGC 253, we carried out additional experiments by adding artificial "stars" to our frames. For this purpose we generated 1000 artificial stars distributed at random in each frame, with magnitudes uniformly distributed over the interval $19 < m < 25$ and identical colors, $(U - B) = (B - V) = 0.0$, for all of them. The transformation coefficients discussed in Sect. 2 were used to transform magnitudes into number counts, and the PSF used for the fit of the photometry in each frame was assigned to the artificial stars. No additional Poisson noise was added to the counts produced by artificial stars, as it may be safely neglected in front of the dominating sky noise at the faint magnitudes of interest. PSF-fitting photometry was then perfomed on the new images in an identical way as with the original images, and a catalog was generated yielding for each artificial star its input magnitude and the recovered one.

Figure 8 shows the distribution of the standard deviation in the recovered magnitudes of the artificial stars, calculated in bins of 0.4 mag. It should be noted that the errors are now calculated from the differences between the "true", i.e., input magnitudes of the artificial stars and the recovered magnitudes, and not from the estimated errors in the fitting of the PSF as was done in the case of the real sources. The procedure thus leads to a more robust estimate of the actual errors. No significant differences are found among the different fields, with the exception already noted in Sect. 2 affecting one of the halo fields in the B filter. This rules out the possibility that the "blue tail" of Fig. 7 may be due to underestimated errors in some of the halo fields, leading one to attribute an error in $B - V$ of less than 0.2 mag to objects whose magnitude uncertainty is actually well above that value. Indeed, should such an underestimate be present, objects with underestimated errors would blur the blue edge of the color distribution of Fig. 2 producing the observed blue tail. Our numerical experiments with artificial stars suggest that this is not the case. This conclusion is reinforced when producing histograms analogous to those of Fig. 7, but now using instead the artificial stars found in the same magnitude interval. Note that the $(B-V) = 0.0$ color of the artificial stars is chosen so as to lie near the edge of the distribution of colors in the control fields, so that the spread due only to photometric errors in this critical color range can be best assessed. The histogram of recovered colors is shown in Fig. 9, where again no apparent differences are found between halo and control fields. Our conclusion from these experiments is thus that there are no spurious effects present in our data that could bias the color distribution of halo objects producing the reported blue tail.

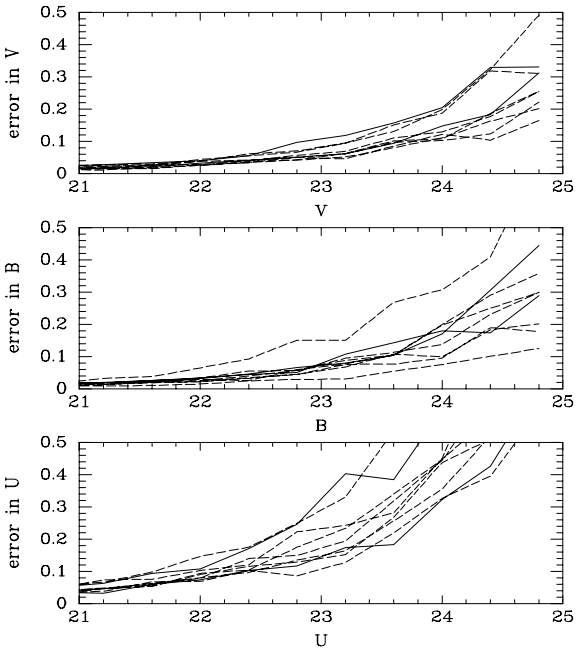

Fig. 8. Standard deviation as a function of the input magnitude of artificial stars introduced in each field. The solid lines correspond to the control fields, and the dotted lines to the halo fields

To obtain a more quantitative estimate on the significance of the excess of blue sources, we have applied the two-sample Kolmogorov-Smirnov test to the samples of point sources in both the halo and the control fields, both in the interval $23 < V < 24.5$ and in other magnitude intervals. In the $23 < V < 24.5$ interval and covering the entire range of $B - V$ colors, the test indicates that both samples are indeed drawn from different underlying distributions to a confidence level $> 99\%$. This level decreases as we consider objects within progressively redder magnitude limits: taking only stars with $B - V > 0$, both samples are found to be different at only a 92% level, despite of the fact that this limit excludes only 79 out of the 862 members of the entire halo sample, and 7 out of 243 members of the control fields sample. The confidence level drops below 90% level if we include only stars with $B - V > 0.2$, and becomes rapidly smaller as we move to redder and redder objects, now partly due to the rapid drop in the number of objects that are detected at B for a given V. Therefore, it is clear that the difference in the $B - V$ color distributions between halo and

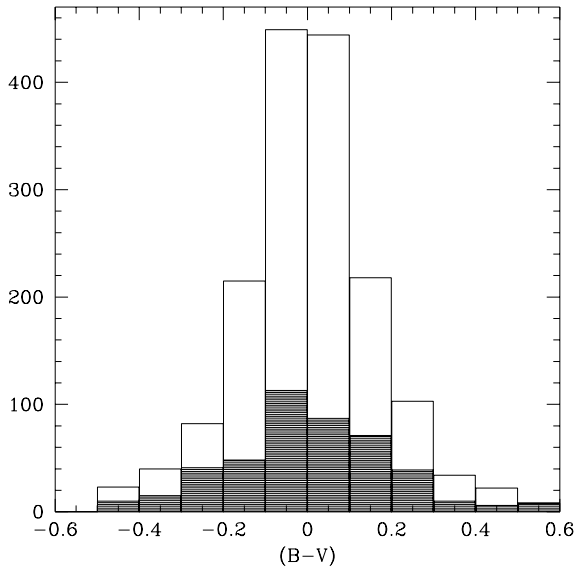

Fig. 9. Same as Fig. 7, but now calculated from the artificial stars introduced in each field. All the artificial stars have input colors $(B-V)=0.0$. No significant differences are found between the halo and the control fields concerning the distribution of recovered colors of the artificial stars

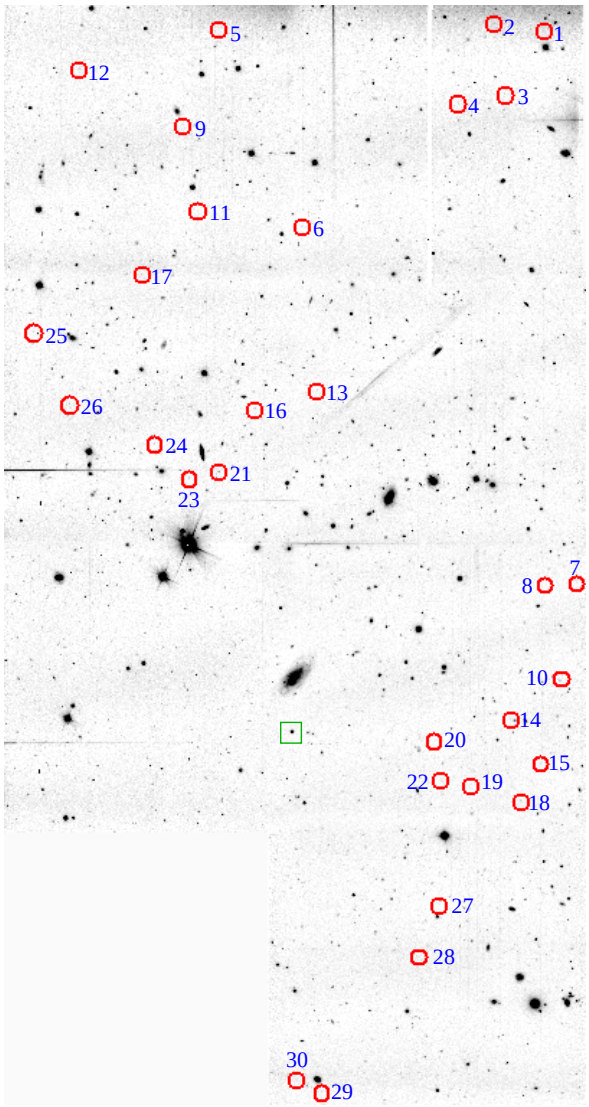

Fig. 10. The V-band mosaic of the halo fields observed with the NTT, showing the positions of the bluest stars detected (circles). The location of the field with respect to NGC 253 is outlined in Fig. 1. The numbering corresponds to the entries in Table 2. The star marked with a square below the center of the image is the $V=18.36$ candidate white dwarf

control fields is a significant one, and that it lies in the blue tails of both distributions. Such an excess of sources at a given color is seen only in that V magnitude range: in other regions of the $(B-V),V$ diagram the significance of the differences never exceeeds 90%. It is remarkable that the difference between both distributions appears in a region where the photometric errors are largest: the effect of such photometric errors should be a dilution of the signal caused by a real excess of blue sources, rather than the creation of a spurious one. Thus, it may be expected that the Kolmogorov-Smirnov test would yield an even higher confidence level if applied on the same sample but with improved photometry.

We have repeated this same exercise using the $(U-B),V$ diagram. In this case we selected only objects having an error in $U-B$ below 0.2 mag, that is, the same uncertainty threshold as for the sample considered so far for the $(B-V),V$ diagram. No significant difference is found now at any V magnitude interval. This is at least partly due to the reduced sensitivity of the test to actual differences arising from the smaller size of the samples, and may also be contributed by the fact that, while blue stars and QSOs can have similar $U-B$ colors, blue stars tend to be bluer than QSOs in $B-V$ at a given $U-B$.

4.2. Location of the blue sources

While statistics clearly shows the signature of an excess of blue objects in the halo of NGC 253 as compared to the control fields, we cannot claim yet that this alone supports the existence of a young stellar component found in the halo of the galaxy. We have already considered in Sect. 3.3 the possibility that post-AGB stars of NGC 253 appear in the bluest part of the $(B-V),V$ diagram as a result of the combination of their intrinsically blue colors and of photometric errors. Moreover, some Population I stars are in fact expected to exist in the innermost regions of the halo, but having formed in the galactic disk and having been expelled to large distances from the plane as runaway stars. Nearly all the halo Population I stars that have been detected in the halo of the Milky Way can be explained in that way (Rolleston 1999).

Given the presently available information, the spatial distribution of the bluest sources may be expected to yield some clues on their nature. To obtain a sample of blue objects as uncontaminated by photometric errors as possible, we have taken only halo objects for which we

measure $B-V<-0.1$ with an error in that color of 0.2 mag or below. We have excluded the very blue source at $V=18.36$ that, as was discussed in Sect. 3.1, is most likely a foreground white dwarf. The space distribution of the 30 sources fulfilling this criterion in the surveyed field is shown in Fig. 10.

Needless to say, a firm interpretation of Fig. 10 is limited by the incomplete coverage of the halo of NGC 253 and by the small number of objects. However, we note that the objects do not appear to be evenly distributed across the field and that they are not concentrated towards the galaxy either. Rather, two distinct groups appear: one roughly occupying the top half of Fig. 10, and another one forming a strip running from top right to bottom center of the lower half of the figure.

Table 2 gives the UBV photometry of the objects plotted in Fig. 10, as well as their projected distances to the plane of the galaxy. Many objects are found at projected distances of a few kpc, consistent with them being early-type runaway stars. However, the second group referred to above has its base at $\simeq$9 kpc from the plane, and its members can be found at the largest projected distances covered in our observations, nearly 15 kpc. Such distances are far too large to be due to a runaway ejection from the plane of the galaxy (even allowing for a 30% variation in these values due to the uncertainty in the distance modulus), as they imply too long a travel time. As a rough estimate, we have assumed that a gravitational potential of the form proposed by Allen & Santillán (1991) for the disk of the Milky Way provides an acceptable representation of that of NGC 253 too, and have adopted the force law perpendicular to the galactic plane given by that model at the solar circle (Table 3 of Allen & Santillán 1991). Using this model, we find that an ejection velocity of at least 400 km s^{-1} would be needed to reach a distance of 10 kpc during the $\sim$3 10^7 yr main-sequence lifetime of a B3 star (Schaller et al. 1992), and more than 600 km s^{-1} for a distance of 15 kpc. These estimates are almost independent on the chosen potential given the short time available for deceleration, and change little even in the limiting case in which no deceleration due to the galactic gravitational potential is taken into account. Such velocities are well above the fastest observed among galactic runaway stars. In a numerical investigation of the maximum possible ejection velocity of stars in a cluster, Leonard (1991) concludes that high velocities like the ones required by a runaway origin in the present case are not only extremely unlikely, but also require an unrealistic mass function of the parent cluster. Moreover, the spectral types of the blue objects found here, as estimated from their absolute magnitudes at the distance of NGC 253, are early B. At these and later B spectral types the fraction of runaway stars is observed to quickly decrease as compared to O type stars, possibly as a consequence of the large mass transfer onto them by the primaries in the binary supernova explosion scenario (Stone 1987; Vanbeveren et al. 1998), so B-type runaway stars are rare. For all these reasons, it thus seems that we can safely exclude a runaway origin for these most distant stars.

Table 2. Identifications, photometry, and projected distances of objects in the halo of NGC 253 having measured $B-V<-0.1$

No.	V	$U-B$	$B-V$	z (kpc)
1	24.08 ± 0.15	-0.83 ± 0.23	-0.21 ± 0.18	2.6
2	23.63 ± 0.10	-0.67 ± 0.19	-0.24 ± 0.14	2.5
3	23.87 ± 0.13	-0.70 ± 0.17	-0.37 ± 0.15	3.4
4	24.31 ± 0.15	-0.98 ± 0.23	-0.13 ± 0.19	3.5
5	24.18 ± 0.15		-0.10 ± 0.20	2.6
6	24.34 ± 0.14	-0.55 ± 0.34	-0.15 ± 0.19	4.9
7	23.89 ± 0.11	-0.75 ± 0.21	-0.16 ± 0.14	9.0
8	24.18 ± 0.11	-0.42 ± 0.28	-0.12 ± 0.15	9.1
9	23.49 ± 0.09		-0.13 ± 0.12	3.7
10	24.48 ± 0.12	-1.19 ± 0.22	-0.11 ± 0.17	10.1
11	24.30 ± 0.14	-0.64 ± 0.30	-0.12 ± 0.19	4.7
12	23.45 ± 0.09	-0.89 ± 0.15	-0.22 ± 0.11	3.1
13	24.06 ± 0.14	-0.80 ± 0.36	-0.17 ± 0.19	6.8
14	23.91 ± 0.09	-0.88 ± 0.18	-0.13 ± 0.12	10.6
15	24.49 ± 0.11		-0.11 ± 0.17	11.1
16	23.46 ± 0.10	-0.53 ± 0.21	-0.18 ± 0.12	7.0
17	24.18 ± 0.15	-0.70 ± 0.29	-0.14 ± 0.19	5.4
18	23.48 ± 0.07	-0.47 ± 0.18	-0.16 ± 0.09	11.6
19	24.62 ± 0.14		-0.18 ± 0.18	11.4
20	24.13 ± 0.12	-1.06 ± 0.19	-0.13 ± 0.15	10.9
21	24.19 ± 0.16	-0.95 ± 0.24	-0.46 ± 0.19	7.7
22	24.18 ± 0.12	-0.94 ± 0.24	-0.13 ± 0.16	11.3
23	23.95 ± 0.13	-0.73 ± 0.24	-0.14 ± 0.14	7.8
24	24.20 ± 0.16	-0.77 ± 0.30	-0.20 ± 0.20	7.4
25	24.55 ± 0.17	-0.26 ± 0.46	-0.23 ± 0.20	6.1
26	24.40 ± 0.18	-0.69 ± 0.29	-0.31 ± 0.20	7.0
27	24.48 ± 0.12		-0.39 ± 0.17	12.8
28	24.46 ± 0.14		-0.12 ± 0.20	13.4
29	24.62 ± 0.14		-0.30 ± 0.18	14.9
30	24.42 ± 0.18	-0.92 ± 0.30	-0.12 ± 0.17	14.8

An alternative possibility, namely that these objects are post-AGB stars, also appears to be very unlikely in view of their space distribution. Post-AGB stars should trace the density distribution of their parental population and, although their presence at the large distances from the disk of NGC 253 such as the ones sampled here is not impossible, their numbers should decrease as one proceeds outwards from the galaxy. Such a decrease is not observed: blue objects are roughly equally abundant in the group near the galaxy (projected distances <8 kpc) as in the more distant group. We note that the same argument rules out a possible contamination by field blue stragglers, about whose origin and properties little is known (Shields & Twarog 1988; Stryker 1993; Royer 1999). This does not imply that our sample does not contain possible post-AGB stars which, together with runaway stars, may contribute at least a fraction of the blue objects near the base of the halo. We rather conclude that the more distant group is almost certainly not composed by those two kinds of objects, as either they should be much more abundant

at smaller projected distances (in the case of post-AGB stars), or they should have been ejected from the disk at unrealistically high velocities (in the case of runaways).

4.3. Star formation in the halo of NGC 253

As discussed in the previous sections, the group of blue objects that we detect at projected distances between 9 and 15 kpc from the disk of NGC 253 cannot be explained, it seems, in terms of any foreground, background, or intrinsic population of NGC 253 not involving recent star formation in the halo of the galaxy. The ranges of colors and magnitudes of the objects that we find in this group are, within the uncertainties, consistent with them being main sequence stars with spectral types B0-B2 at the distance of NGC 253.

An independent support for the existence of this population would be the discovery of a *reservoir* of cold gas providing possible star formation sites in the halo of NGC 253. This would be the analogous to the HVC system of our Galaxy, while their detection in association with NGC 253 would allow a direct measurement of their masses and average densities (not possible so far for our own Galaxy due to the lack of reliable distance indicators to HVCs) thus allowing an estimate of their star forming potential. A spatial coincidence between a HI cloud in NGC 253 and our detected blue objects would strongly reinforce the picture proposed here of star formation in the halo of that galaxy. However, it is unfortunate that no deep, sensitive, high resolution search for HI in the halo of NGC 253 has been published to date. We have tried to find evidence for HI clouds in the halo of NGC 253 using the recently published HI Parkes All-Sky Survey (Staveley-Smith 2000), but its spatial resolution is too coarse for our purposes. Nevertheless, HI detections in the haloes of other nearby galaxies have been reported (Schulman 1994; Schulman et al. 1996), suggesting that such a component may also be present in the halo of NGC 253.

It is interesting to point out that observations of the halo of NGC 253 in radio continuum, extending to distances from the galactic plane comparable (albeit somewhat smaller) than the ones reported here, have been carried out by Carilli et al. (1992). These observations do not probe cold gas, but synchrotron emission by cosmic rays spiraling around magnetic field lines blown into the halo. Interestingly, those authors find an enhancement of the radio continuum intensity near the position where we find the first objects of the large-distance group (cf. their Fig. 2). It is not possible to see from the data of Carilli et al. if such an enhancement traces the distribution of the rest of blue objects in that region, because their map does not reach to such large distances from the galaxy. The origin of the intensity enhancement is not clear either, and it cannot be ruled out that it might be just a chance alignment of a background radio source. However, the possibility that this enhancement may be due to an increased gas density caused by an obstacle along the path of the radio-emitting material is an intriguing one in the present context. If this were the case, the emerging picture may be reminiscent of that proposed by Graham (1998) for Centaurus A, where a high velocity outflow is encountering denser HI gas and inducing instabilities leading to star formation in the process. Observations of other phases of the interstellar gas probed by other techniques, mainly 21 cm observations of HI, would be essential in confirming this hypothesis.

4.4. Future developments

The observations reported here provide preliminary evidence, mainly of statistical nature, on the existence of ongoing star formation in the halo of NGC 253. To put this evidence on a firmer standing new observations, well within present capabilities, are needed. Here we outline a few that can be easily pursued.

A necessary first step is to photometrically and spectroscopically confirm the Population I nature of the blue sources reported here. As has been noted, these objects appear in regions of the color-magnitude diagram where the photometric error bars are already considerable, becoming comparable or even larger than the color gap separating early-type stars from other, redder objects that are not of direct interest in the present study. Some objects that we have classified as possible blue halo stars here (including the best candidates listed in Table 2) may actually have redder colors than the ones listed here, while some objects with actual colors bluer than the cutoff proposed in Sect. 4.2 may not have been selected due to photometric errors.

Spectroscopy would help in cleaning our sample from unrelated background contamination, as quasars would appear clearly distinct from main sequence Population I objects even in low resolution, low signal-to-noise spectra. The same cannot be said however about the possibility of spectroscopically separating early-type Population I objects from post-AGB stars: even high resolution, high signal-to-noise spectra obtained for much brighter objects in our own Galaxy have been unable to provide a definitive answer on the character of some objects until detailed atmospheric abundance analyses have been performed (Hambly et al. 1997). In this respect, improved photometry at faint magnitudes may allow to largely disentangle both kinds of objects, which should cluster along two different sequences in the $(B-V), V$ diagram: Population I stars should become fainter when going to redder colors, while the opposite should happen to post-AGB stars due to the increasing bolometric correction at bluer colors. The photometric uncertainty in the present sample prevents nevertheless the disentangling of those two sequences. For the time being, statistical arguments on the spatial distribution of sources such as those presented above may be expected to provide the ultimate support for the real Population I character of the blue objects most distant from NGC 253.

Although the area observed by us covers a considerable fraction of the halo of NGC 253, the results are somewhat tantalizing in this respect. What is the real extent of the group of blue sources far from the halo of NGC 253? Are there other such groups elsewhere in the halo of that galaxy? Wider field imaging of the halo of NGC 253 is needed to answer these questions and to provide a better assessment on the importance of star formation there. If in situ massive star formation is taking place in other locations of the halo of the galaxy, it is possible that earlier-type objects than those tentatively identified in the present work may be found. Such earlier objects should be brighter than the ones detected so far, thus removing any remaining possibility of confusion with post-AGB stars in NGC 253. Another important motivation for these observations would be to correlate the position of possible groups of blue objects in the halo with structures in the center or the disk of NGC 253, mainly the central starburst and the abundant chimney-like structures identified in the disk by Sofue et al. (1994). In our case, the location of the group of blue objects at a large distance from the galaxy almost directly below the center of the galaxy (taking as a reference the direction defined by the perpendicular to the plane of the galaxy) is suggestive of a direct relation between the energetic activity of the central starburst and the formation of those stars.

As already mentioned, HI observations of the halo of NGC 253 are needed to reveal the sites where the identified blue stars may have been formed. Hα imaging may also reveal the connections between the blue objects and their parental gas, as seems to be the case of Centaurus A (Graham 1998). However, the derived spectral types of the candidate blue stars reported here are not early enough to produce HII regions visible at that distance. Such observations should be tried however if the wide field imaging suggested above revealed earlier spectral types.

5. Summary and conclusions

We have presented deep UBV observations of an area of 198 arcmin^2 in the direction of the edge-on starburst galaxy NGC 253, corresponding to a projected distance ranging from 2.3 to 15 kpc from the plane of the galaxy. Our goal is to identify a possible blue population of objects with characteristics consistent with them being normal early-type Population I stars at the distance of NGC 253. We have also imaged to the same depth two control fields in a nearby direction, in order to directly estimate the contribution of the foreground and the background to the object counts at different colors and magnitudes. Our conclusions can be summarized as follows:

- The overall distribution of object counts in color-color and color-magnitude diagrams agrees well with what is expected from a field dominated by background and foreground objects, unrelated to the halo of NGC 253. In particular, the disk and spheroid components of the Milky Way are well visible in the $(B-V), V$ diagram at the brighter magnitudes, while extragalactic objects dominate at fainter magnitudes;
- Foreground galactic objects (hot subdwarfs, blue horizontal branch stars, and white dwarfs) are expected to yield a negligible contribution to the counts of blue sources ($(B-V) < 0$) in the direction of NGC 253, based on predictions of starcount models and large area surveys. This is confirmed by the observations of the halo fields;
- The main contribution to faint object counts at blue magnitudes is expected to come from intrinsically blue QSOs with strong emission lines and $z < 2.3$. Faint objects with $V > 23$, $(B-V) < 0.5$ are indeed abundant both in the halo and control fields, although they are rarely found with $(B-V) < 0$, especially in the control fields;
- An excess of blue objects with $V > 23$ and $(B-V) < 0$ is found in the halo fields when compared to the control fields. A Kolmogorov-Smirnov test shows that the difference between the $(B-V)$ color distributions of the halo and control fields is significant to a level above 99%, but this level drops rapidly when only objects with $(B-V) > 0$ are considered. Thus, it is clear that the difference lies in the existence of a blue tail in the distribution of colors of faint halo objects, that is replaced by a rather sharp cutoff near $(B-V) = 0$ in the control fields;
- The possibility that the excess of faint blue objects in the halo of NGC 253 is caused by bright post-AGB stars in that galaxy is considered as very unlikely on the basis of absolute magnitude and positional arguments. The latter also apply to the possibility that those objects are field blue stragglers of NGC 253. Therefore, we favour the interpretation of these objects as being Population I stars in the halo of NGC 253. The spectral types inferred from their absolute magnitudes are B0-B2;
- The bluest objects detected in the halo of NGC 253 appear to belong to two distinct spatial groups, with different projected distances to the plane of the galaxy. One of them, extending up to 8 kpc of projected distance, may contain runaway stars of NGC 253. The other group starts at 9 kpc and forms a strip reaching up to the largest projected distances (15 kpc) covered by our observations. Stars in this latter group are extremely unlikely to be runaway, given the very large high velocities that would be required for them to reach such large distances from the disk. We therefore conclude that, if the Population I nature of these objects is confirmed, they provide direct evidence for the existence of present-day star formation in the halo of NGC 253;
- The base of the strip of distant blue halo objects is spatially coincident with a peak in the distribution of 20 cm radio continuum emission due to cosmic rays flowing into the halo of NGC 253. We propose that this peak might be due to the collision of hot gas from the superwind generated at the nuclear starburst of

NGC 253 with a denser HI cloud of the halo. The compression of this cloud would cause star formation, much in the way that has been proposed to explain star formation in a HI cloud associated to Centaurus A;
– More observations are needed to confirm the existence of a Population I component of the halo of NGC 253 and to investigate its origin. Among them we can list higher precision photometry, spectroscopy of the blue objects, wide-area surveys of a larger portion of the halo and of control fields, and sensitive high resolution HI observations of the halo.

Acknowledgements. We are pleased to thank the NTT Team in ESO-La Silla for excellent support during our observations, especially Dr. Vanessa Doublier and Mr. Jorge Miranda. Our thanks also to Dr. Alvio Renzini for useful remarks on the possible detectability of post-AGB stars in the halo of NGC 253. The careful reading and useful suggestions of the anonymous referee, especially concerning testing the behaviour of photometric errors at faint magnitudes, contributed to improve this paper and are gratefully acknowledged.

References

Alcaino, G., & Liller, W. 1984, AJ, 89, 814
Allen, S. W. 1995, MNRAS, 276, 947
Allen, C., & Santillán, A. 1991, RMxA&A, 22, 255
Barmby, P., Huchra, J. P., Brodie, J. P., et al. 2000, AJ, 119, 727
Best, P. N., Longair, M. S., & Röttgering, H. J. A. 1997, MNRAS, 292, 758
Bond, H. E., & Fullton, L. K. 1997, A&AS, 190, 4703
Braccesi, A., Zitelli, V., Bònoli, F., & Formiggini, L. 1980, A&A, 85, 80
van Breugel, W. J. M., & Dey, A. 1993, ApJ, 414, 563
van Breugel, W., Filippenko, A. V., Heckman, T., & Miley, G. 1985, ApJ, 293, 83
Brown, P. J. F., Dufton, P. L., Keenan, F. P., et al. 1989, ApJ, 339, 397
Carilli, C. L., Holdaway, M. A., Ho, P. T. P., & De Pree, C. G. 1992, ApJ, 399, L59
Castelli, F. 1999, A&A, 346, 564
Charmandaris, V., Combes, F., & van der Hulst, J. M. 2000, A&A, 356, L1
Christodoulou, D. M., Tohline, J. E., & Keenan, F. P. 1997, ApJ, 486, 810
Combes, F., & Charmandaris, V. 2000, A&A, in press
Conlon, E. S., Dufton, P. L., Keenan, F. P., McCausland, R. J. H., & Holmgren, D. 1992, ApJ, 400, 273
Conti, A., Kennefick, J. D., Martini, P., & Osmer, P. S. 1999, AJ, 117, 645
Crawford., C. S., & Fabian, A. C. 1993, MNRAS, 265, 431
Cristiani, S., Barbieri, C., Iovino, A., La Franca, F., & Nota, A. 1989, A&AS, 77, 161
Davidge, T. J., & Pritchet, C. J. 1990, AJ, 100, 102
Davidge, T. J., Le Fevre, O., & Clark, C. C. 1991, ApJ, 370, 559
Demers, S., Grondin, L., Irwin, M. J., & Kunkel, W. E. 1991, AJ, 101, 911
Donahue, M., Aldering, G., & Stocke, J. T. 1995, ApJ, 450, L45
Dorman, B., Rood, R. T., & O'Connell, R. W. 1993, ApJ, 419, 596
Dyson, J. E., & Hartquist, T. W. 1983, MNRAS, 203, 1233
Elson, R. A. W., Santiago, B. X., & Gilmore, G. F. 1996, New Astr., 1, 1
Graham, J. A. 1982, ApJ, 252, 474
Graham, J. A. 1998, ApJ, 502, 245
Grondin, L., Demers, S., & Kunkel, W. E. 1992, AJ, 103, 1234
Hall, P. B., Osmer, P. S., Green, R. F., Porter, A. C., & Warren, S. J. 1996, ApJ, 462, 614
Hambly, N. C., Conlon, E. S., Dufton, P. L., et al. 1993, ApJ, 417, 706
Hambly, N. C., Fitzsimmons, A., Keenan, F. P., et al. 1995, ApJ, 448, 628
Hambly, N. C., Dufton, P. L., Keenan, F. P., & Lumsden, S. L. 1996, MNRAS, 278, 811
Hambly, N. C., Rolleston, W. R. J., Keenan, F. P., Dufton, P. L., & Saffer, R. A. 1997, ApJS, 111, 419
Hoopes, C. G., Walterbos, R. A. M., & Rand, R. J. 1999, ApJ, 522, 669
Ibata, R. A., Richer, H. B., Gilliland, R. L., & Scott, D. 1999, ApJ, 524, L95
Ivezic, Z., & Christodoulou, D. M. 1997, ApJ, 486, 818
Landolt, A. U. 1992, AJ, 104, 340
Lehnert, M. D., & Heckman, T. M. 1995, ApJS, 97, 89
Lehnert, M. D., & Heckman, T. M. 1996, ApJ, 462, 651
Leonard, P. J. T. 1991, AJ, 101, 562
Little, J. E., Dufton, P. L., Keenan, F. P., et al. 1995, ApJ, 447, 783
Mac Low, M.-M. 1999, in New Perspectives on the Interstellar Medium, ASP Conf. Ser., 168
Méndez, R. A. 1995, Ph.D. Thesis, Yale University
Méndez, R. A., & Minniti, D. 2000, ApJ, 529, 911
Méndez, R. A., Minniti, D., de Marchi, G., Baker, A., & Couch, W. J. 1996, MNRAS, 283, 666
Mendoza, E. E., & Arellano Ferro, A. 1993, AJ, 106, 2524
Moehler, S., & Heber, U. 1998, A&A, 335, 985
Parthasarathy, M. 1993, ApJ, 414, L109
Pinkney, J., Holtzman, J., Garasi, C., et al. 1996, ApJ, 468, L13
Pildis, R. A., Bregman, J. N., & Schombert, J. M. 1994, ApJ, 427, 160
Puche, D., & Carignan, C. 1988, AJ, 95, 1025
Rolleston, W. R. J., Hambly, N. C., Dufton, P. L., et al. 1997, MNRAS, 290, 422
Rolleston, W. R. J., Hambly, N. C., Keenan, F. P., Dufton, P. L., & Saffer, R. A. 1999, A&A, 347, 69
Rossa, J., & Dettmar, R.-J. 2000, A&A, 359, 433
Royer, F. 1999, Ph.D. Thesis, Observatoire de Paris
Scannapieco, E., Ferrara, A., & Broadhurst, T. 2000, ApJ, 536, L11
Schaller, G., Schaerer, D., Meynet, G., & Maeder, A. 1992, A&AS, 96, 269
Schiminovich, D., van Gorkom, J. H., van der Hulst, J. M., & Kasow, S. 1994, ApJ, 423, L101
Schmidt-Kaler, T. 1982, in Landolt-Börnstein, vol. 2b, ed. J. Schaifers, & H. H. Voigt (Springer-Verlag)
Scholz, R.-D., Meusinger, H., & Irwin, M. 1997, A&A, 325, 457
Schulman, E., Bregman, J. N., & Roberts, M. S. 1994, ApJ, 423, 180
Schulman, E., Bregman, J. N., Brinks, E., & Roberts, M. S. 1996, AJ, 112, 960
Shields, J. C., & Twarog, B. A. 1988, ApJ, 324, 859
Sluis, A. P. N., & Arnold, R. A. 1998, MNRAS, 297, 732
Smith, E. P., Bohlin, R. C., Bothun, G. D., et al. 1997, ApJ, 478, 516

Sofue, Y., Wakamatsu, K.-I., & Malin, D. F. 1994, AJ, 108, 2102
Staveley-Smith, L. 2000, in Imaging at radio through submillimeter wavelengths, ASP Conf. Ser., in press
Stetson, P. B. 1987, PASP, 99, 191
Stobie, R. S., & Ishida, K. 1987, AJ, 93, 642
Stone, R. C. 1979, ApJ, 232, 520
Stryker, L. L. 1993, PASP, 105, 1081
Tully, R. B. 1988, Nearby Galaxies Catalogue (Cambridge Univ. Press)
Vanbeveren, D., De Loore, C., & Ven Rensbergen, W. 1998, A&AR, 9, 63
Villeneuve, B., Wesemael, F., & Fontaine, G. 1995, ApJ, 450
Wakker, B. P., & van Woerden, H. 1997, ARA&A, 35, 217
Yoshii, Y., Ishida, K., & Stobie, R. S. 1987, AJ, 93, 323